

Carbon flows and biochar stability during co-pyrolysis of human faeces with wood biomass

M.E. Koulouri*, M. Qiu, M.R. Templeton, G.D. Fowler

Department of Civil and Environmental Engineering, Imperial College London, UK, SW7 2AZ

Keywords: human excreta, faecal sludge, carbon sequestration, carbon storage, container-based sanitation

*Corresponding author email: maria.koulouri17@imperial.ac.uk

Supplementary Information

1. Lab-scale pyrolysis rotary furnace

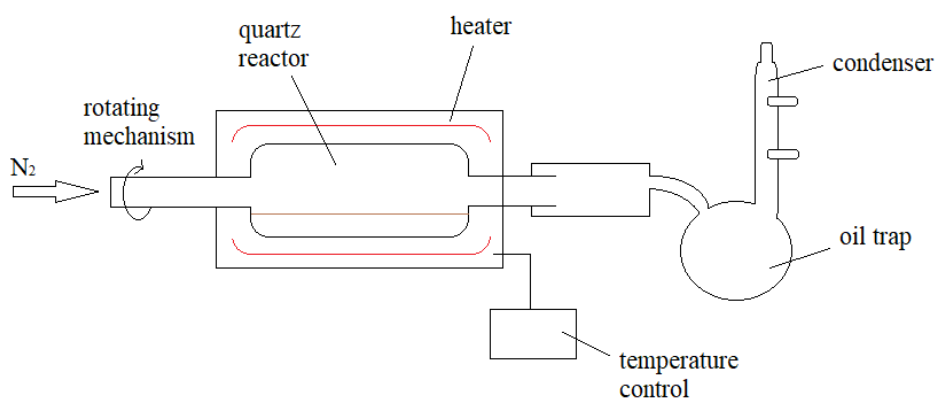


Figure S1: Experimental pyrolysis set up (Roger Perry Laboratory, Imperial College London).

2. Thermogravimetric analysis of HF, HF50 and WB

The thermal decomposition behaviour of samples HF, HF50 and WB is depicted in the thermogravimetric analysis (TGA) and derivative thermogravimetry (DTG) curves shown in **Figure S2**. For all samples a first weight loss peak is observed at around 80 °C and completed by 150 °C, due to drying and dehydration reactions. The maximum rate of decomposition is noticed at 310 °C, 335 °C and 345 °C for HF, HF50 and WB respectively. The earlier peak weight loss rate for faeces compared to wood can be attributed to the decomposition of protein¹. Main pyrolysis reactions are complete by 500-550 °C for HF, HF50 and 450-500 °C for WB. A distinct shoulder peak is observed for HF at 400-500 °C which has also been observed for previous studies² and is attributed to the decomposition of oil and grease³. Notably, this shoulder peak is not observed for WB, which shows a distinct single peak associated with lignin and cellulose/hemicellulose decomposition. Further weight loss is observed after 700 °C due to continued carbonisation, particularly for HF which show a weight loss peak at 850°C.

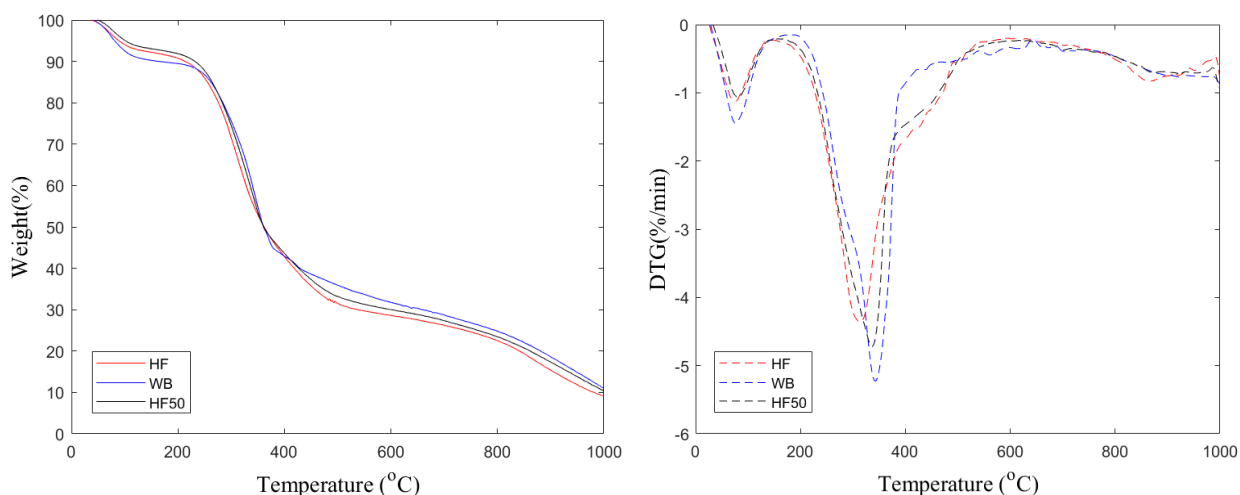


Figure S2: TGA and DTG curves for human faeces (HF), wood biomass (WB) and mixed HF:WB 50:50 (HF50).

3. FTIR spectra for biochar samples B-HF, B-HF75, B-HF50, B-HF25, B-WB

The Fourier Transform Infrared Spectroscopy (FTIR) spectra for samples B-HF, B-HF75, B-HF50, B-HF25 and B-WB are shown in **Figure S3**. The peaks at $\sim 1600\text{-}1500\text{ cm}^{-1}$ associated with C=C stretching were stronger for samples containing more WB and are indicative of lignin and aromatic carbon⁴. Peaks in the $900\text{-}700\text{ cm}^{-1}$ region (C-H bending), associated with mono-, polycyclic and substituted aromatic compounds, were also stronger for the biochars high in WB content, suggesting the enhanced stability of these biochars⁵. On the contrary, strong peaks at $1040\text{-}1020\text{ cm}^{-1}$ and 550 cm^{-1} which have been associated with carbohydrates and phosphates, were more intense for the biochars containing more HF and almost eliminated for B-HF25^{3,6}. The presence of carbonates was also confirmed by the strong peaks at $\sim 1030\text{ cm}^{-1}$ as well as peaks at 870 cm^{-1} and vibrations at $1500\text{-}1300\text{ cm}^{-1}$ ⁷. Bands between wavenumbers $4000\text{-}2000\text{ cm}^{-1}$ showing C-H and O-H stretching regions are not shown, due to the limited differences observed between samples and the signal noise due to the presence of moisture.

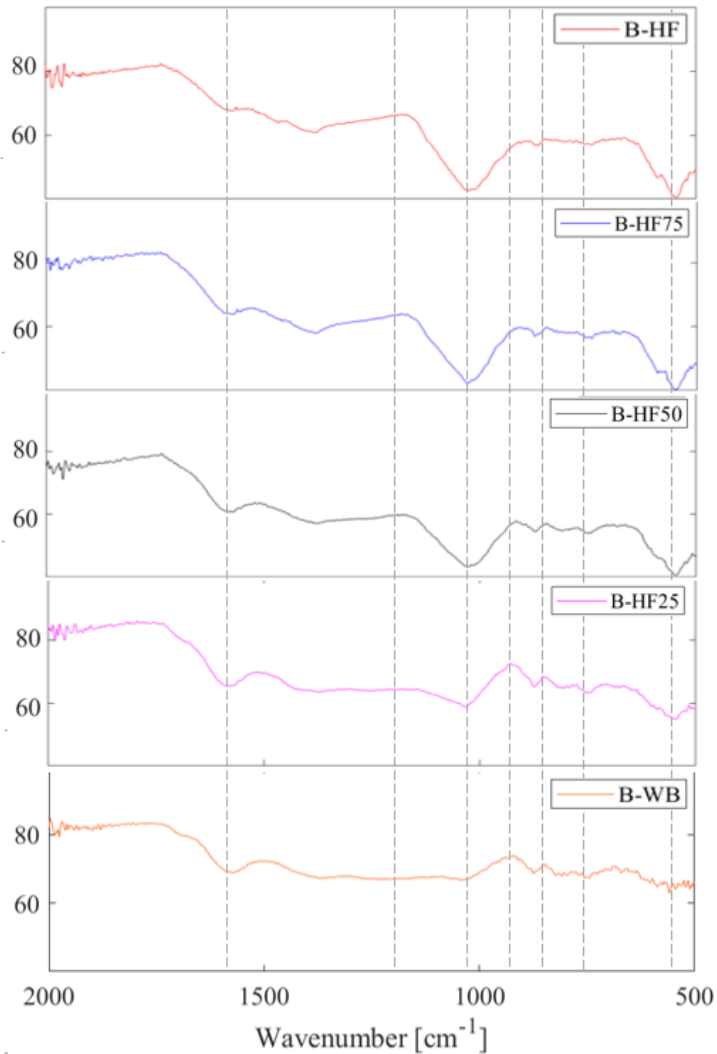


Figure S3: Fourier-transform infrared spectroscopy (FTIR) spectra for biochars B-HF, B-HF75, B-HF50, B-HF25 and B-WB produced at 550°C.

4. Biochar yield during pyrolysis

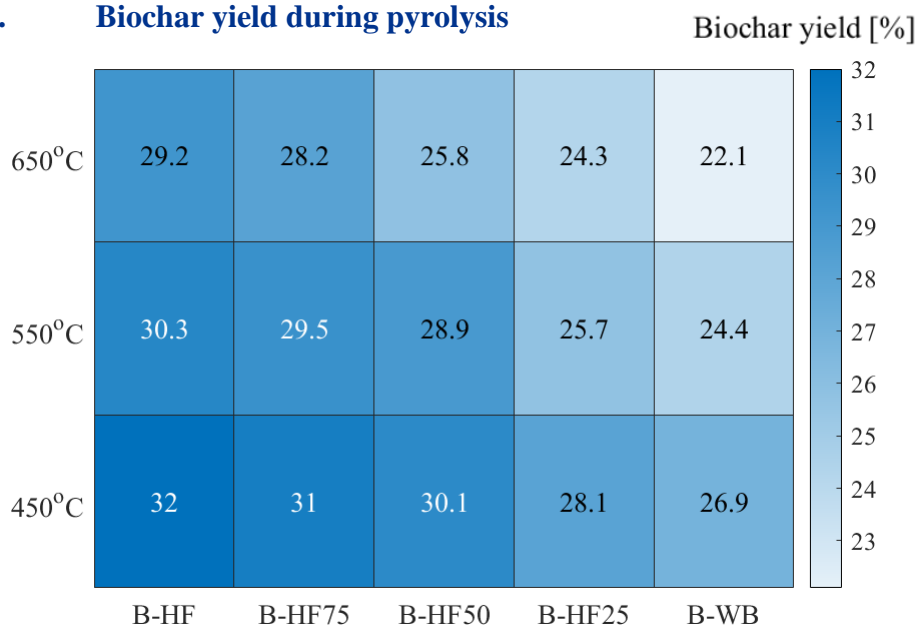


Figure S4: Biochar yield for B-HF, B-HF75, B-HF50, B-HF25 and B-WB produced at 450°C, 550°C, 650°C.

5. Statistical analysis results

Table S1: p-values of one-way ANOVA for differences in feedstock C and proximate analysis results, with changes in HF:WB blending ratio (HF, HF75, HF50, HF25, WB) (**bold** for significant differences $p < 0.05$).

	C	VM	FC	Ash
HF vs. HF75	0.1314	0.7497	<0.001	<0.001
HF vs. HF50	0.0344	0.0819	<0.001	<0.001
HF vs. HF25	0.0226	0.0577	<0.001	<0.001
HF vs. WB	0.0159	0.0397	<0.001	<0.001
HF75 vs. HF50	0.008	<0.001	<0.001	0.0014
HF75 vs. HF25	0.0097	<0.001	<0.001	<0.001
HF75 vs. WB	0.0086	0.0025	<0.001	<0.001
HF50 vs. HF25	0.1963	0.3731	0.0098	0.0066
HF50 vs. WB	0.0739	0.1554	<0.001	<0.001
HF25 vs. WB	0.3608	0.2476	0.0011	0.0011

Table S2: p-values of two-way ANOVA for differences in biochar yield, proximate analysis and dissolved organic carbon (DOC) results, with changes in pyrolysis temperature (450, 550, 650 °C) and HF:WB ratio (B-HF, B-HF75, B-HF50, B-HF25, B-WB) (**bold** for significant differences $p < 0.05$).

ANOVA table					
	Yield	VM	FC	Ash	DOC
Pyrolysis temperature	<0.001	<0.001	<0.001	<0.001	<0.001
HF:WB ratio	<0.001	<0.001	<0.001	<0.001	<0.001
Interaction	0.0278	<0.001	<0.001	<0.001	<0.001
Multiple comparison test - Pyrolysis temperature					
450-550	<0.001	<0.001	<0.001	<0.001	<0.001
450-650	<0.001	<0.001	<0.001	<0.001	<0.001
550-650	<0.001	<0.001	<0.001	<0.001	0.055315
Multiple comparison test – HF:WB ratio					
B-HF vs. B-HF75	0.017679	0.98839	<0.001	<0.001	<0.001
B-HF vs. B-HF50	<0.001	0.03623	<0.001	<0.001	<0.001
B-HF vs. B-HF25	<0.001	0.02035	<0.001	<0.001	<0.001
B-HF vs. B-WB	<0.001	0.00100	<0.001	<0.001	<0.001
B-HF75 vs. B-HF50	<0.001	0.05158	<0.001	<0.001	<0.001
B-HF75 vs. B-HF25	<0.001	0.00992	<0.001	<0.001	<0.001
B-HF75 vs. B-WB	<0.001	<0.001	<0.001	<0.001	<0.001
B-HF50 vs. B-HF25	<0.001	0.95807	<0.001	<0.001	0.2541
B-HF50 vs. B-WB	<0.001	0.37036	<0.001	<0.001	0.0954
B-HF25 vs. B-WB	<0.001	0.77632	<0.001	<0.001	0.9846

Table S3: p-values of one-way ANOVA for differences in biochar stability (H₂O₂ oxidation, R₅₀ recalcitrance index) and carbon retention, with changes in HF:WB blending ratio (B-HF, B-HF75, B-HF50, B-HF25, B-WB) (**bold** for significant differences p<0.05).

Compared HF:WB ratios	H ₂ O ₂ oxidation	R ₅₀ index	Carbon retention
B-HF vs. B-HF75	< 0.001	0.90544	0.00139
B-HF vs. B-HF50	< 0.001	0.02448	< 0.001
B-HF vs. B-HF25	< 0.001	< 0.001	< 0.001
B-HF vs. B-WB	< 0.001	0.00316	< 0.001
B-HF75 vs. B-HF50	< 0.001	0.13885	< 0.001
B-HF75 vs. B-HF25	< 0.001	< 0.001	< 0.001
B-HF75 vs. B-WB	< 0.001	0.02169	< 0.001
B-HF50 vs. B-HF25	0.09070	0.18429	0.62127
B-HF50 vs. B-WB	< 0.001	0.8844	0.73968
B-HF25 vs. B-WB	< 0.001	0.64576	0.09980

Table S4: Two-way ANOVA results for differences in carbon flows to the biochar fraction, with changes in wood addition (HF, HF50, WB) and retention time (0.5, 2 h).

ANOVA table for biochar carbon flows (N₂ flow constant)					
Effect of wood addition & retention time					
	SS	df	MS	F	p-Value
Retention time	5.445	1	5.445	4.4	0.0577
Feedstock type	318.69	2	159.345	128.85	< 0.001
Interaction(time:type)	0.09	2	0.045	0.04	0.9644
Error	14.84	12	1.237		
Total	339.065	17			
Multiple comparison test: Feedstock type (HF, HF50, WB)					
	Lower 95% CI	Mean difference	Upper 95% CI		p-Value
HF vs. HF50	-10.7129	-9	-7.2871		< 0.001
HF vs. WB	-10.5629	-8.85	-7.1371		< 0.001
HF50 vs. WB	-1.5629	0.15	1.8629		0.9704

Table S5: Two-way ANOVA results for differences in carbon flows to the biochar fraction, with changes in wood addition (HF, HF50, WB) and N₂ gas flow rate (0.5, 1.5 L/min).

ANOVA table for biochar carbon flows (retention time constant)					
Effect of wood addition & N₂ gas flow rate					
	SS	df	MS	F	p-Value
N ₂ gas flow	37.845	1	37.845	28.03	< 0.001
Feedstock type	144.39	2	72.195	53.48	< 0.001
Interaction(gas:type)	36.39	2	18.195	13.48	< 0.001
Error	16.2	12	1.35		
Total	234.825	17			
Multiple comparison test: Feedstock type (HF, HF50, WB)					
	Lower 95% CI	Mean difference	Upper 95% CI		p-Value
HF vs. HF50	-8.2897	-6.5	-4.7103		< 0.001
HF vs. WB	-7.1397	-5.35	-3.5603		< 0.001
HF50 vs. WB	-0.6397	1.15	2.9397		0.24

Table S6: Two-way ANOVA results for differences in carbon flows to the bio-oil fraction, with changes in wood addition (HF, HF50, WB) and retention time (0.5, 2 h).

ANOVA table for bio-oil carbon flows (N₂ flow constant)					
Effect of wood addition & retention time					
	SS	df	MS	F	p-Value
Retention time	450	1	450	346.6	< 0.001
Feedstock type	196	2	98	75.48	< 0.001
Interaction(time:type)	84	2	42	32.35	< 0.001
Error	15.58	12	1.2983		
Total	745.58	17			
Multiple comparison test: Feedstock type (HF, HF50, WB)					
	Lower 95% CI	Mean difference	Upper 95% CI		p-Value
HF vs. HF50	1.2449	3	4.7551		0.017
HF vs. WB	6.2449	8	9.7551		< 0.001
HF50 vs. WB	3.2449	5	6.7551		< 0.001

Table S7: Two-way ANOVA results for differences in carbon flows to the bio-oil fraction, with changes in wood addition (HF, HF50, WB) and N₂ gas flow rate (0.5, 1.5 L/min).

ANOVA table for bio-oil carbon flows (retention time constant)					
Effect of wood addition & N₂ gas flow rate					
	SS	df	MS	F	p-Value
N ₂ gas flow	722	1	722	613.6	< 0.001
Feedstock type	57	2	28.5	24.22	< 0.001
Interaction(gas:type)	13	2	6.5	5.52	0.0199
Error	14.12	12	5.52		
Total	806.12	17			
Multiple comparison test: Feedstock type (HF, HF50, WB)					
	Lower 95% CI	Mean difference	Upper 95% CI		p-Value
HF vs. HF50	-2.1708	-0.5	1.1708		0.7110
HF vs. WB	1.8292	3.5	5.1708		< 0.001
HF50 vs. WB	2.3292	4	5.6708		< 0.001

Table S8: Two-way ANOVA results for differences in carbon flows to the non-condensable gases (NCG) fraction, with changes in wood addition (HF, HF50, WB) and retention time (0.5, 2 h).

ANOVA table for NCG carbon flows (N₂ flow constant)					
Effect of wood addition & retention time					
	SS	df	MS	F	p-Value
Retention time	612.5	1	612.5	136.67	< 0.001
Feedstock type	124	2	62	13.83	< 0.001
Interaction(time:type)	76	2	38	8.48	0.0051
Error	53.78	12	4.482		
Total	866.28	17			
Multiple comparison test: Feedstock type (HF, HF50, WB)					
	Lower 95% CI	Mean difference	Upper 95% CI		p-Value
HF vs. HF50	2.7392	6	9.2608		0.001
HF vs. WB	-2.2608	1	4.2608		0.6993
HF50 vs. WB	-8.2608	-5	-1.7392		0.0039

Table S9: Two-way ANOVA results for differences in carbon flows to the non-condensable gases (NCG) fraction, with changes in wood addition (HF, HF50, WB) and N₂ gas flow rate (0.5, 1.5 L/min).

ANOVA table for NCG carbon flows (retention time constant)					
Effect of wood addition & N₂ gas flow rate					
N ₂ gas flow	1058	1	1058	233.47	< 0.001
Feedstock type	163	2	81.5	17.98	< 0.001
Interaction(gas:type)	49	2	24.5	5.41	0.0212
Error	54.38	12			
Total	1324.38	17			
Multiple comparison test: Feedstock type (HF, HF50, WB)					
	Lower 95% CI	Mean difference	Upper 95% CI		p-Value
HF vs. HF50	3.7211	7	10.2789		< 0.001
HF vs. WB	-1.7789	1.5	4.7789		0.4642
HF50 vs. WB	-8.7789	-5.5	-2.2211		0.002

References

- 1 M. E. Koulouri, M. R. Templeton and G. D. Fowler, Source separation of human excreta: Effect on resource recovery via pyrolysis, *J. Environ. Manage.*, 2023, **338**, 117782.
- 2 T. Somorin, A. Parker, E. McAdam, L. Williams, S. Tyrrel, A. Kolios and Y. Jiang, Pyrolysis characteristics and kinetics of human faeces, simulant faeces and wood biomass by thermogravimetry–gas chromatography–mass spectrometry methods, *Energy Reports*, 2020, **6**, 3230–3239.
- 3 B. C. Krueger, G. D. Fowler, M. R. Templeton and S. Septien, Faecal sludge pyrolysis: Understanding the relationships between organic composition and thermal decomposition, *J. Environ. Manage.*, 2021, **298**, 113456.
- 4 R. Janu, V. Mrlik, D. Ribitsch, J. Hofman, P. Sedláček, L. Bielská and G. Soja, Biochar surface functional groups as affected by biomass feedstock, biochar composition and pyrolysis temperature, *Carbon Resour. Convers.*, 2021, **4**, 36–46.
- 5 K. Sahoo, A. Kumar and J. Chakraborty, A comparative study on valuable products: bio-oil, biochar, non-condensable gases from pyrolysis of agricultural residues, *Journal of Material Cycles and Waste Management*, 2021, **23**, 186–204.
- 6 W. Jastrzębski, M. Sitarz, M. Rokita and K. Bułat, Infrared spectroscopy of different phosphates structures, *Spectrochim. Acta. A. Mol. Biomol. Spectrosc.*, 2011, **79**, 722–727.
- 7 F. B. Reig, J. V. G. Adelantado and M. C. M. Moya Moreno, FTIR quantitative analysis of calcium carbonate (calcite) and silica (quartz) mixtures using the constant ratio method. Application to geological samples, *Talanta*, 2002, **58**, 811–821.